

## Thermal Development from Hybrid Gels of Compounds for Use in Fibre-Reinforced Oxide Ceramics

Kenneth J. D. MacKenzie\*, Tim Kemmitt, Richard H. Meinhold, Martin Schmücker and Lutz Mayer

New Zealand Institute for Industrial Research and Development,  
P.O. Box. 31-310 Lower Hutt, New Zealand

Chemistry Department, Auckland University, New Zealand,  
Institute of Materials, German Aerospace Center, Köln, Germany

\*Department of Materials, University of Oxford, OX1 3PH, UK.

(Received September 23, 1998)

Mixed oxide compounds of potential usefulness for fibre coatings (hexagonal celsian,  $\text{BaAl}_2\text{Si}_2\text{O}_8$  and lanthanum hexaluminate,  $\text{LaAl}_6\text{O}_{12}$ ) or for matrix materials (yttrium aluminium garnet,  $\text{Y}_3\text{Al}_5\text{O}_{12}$ ) were prepared by hybrid sol-gel synthesis and their thermal crystallisation was monitored by thermal analysis, X-ray diffraction and multinuclear solid state MAS NMR. All the gels convert to the crystalline phase below about 1200°C, via amorphous intermediates in which the Al shows an NMR resonance at 36-38 ppm sometimes ascribed to Al in 5-fold coordination. Additional information about the structural changes during thermal treatment was provided by  $^{29}\text{Si}$ ,  $^{137}\text{Ba}$  and  $^{89}\text{Y}$  MAS NMR spectroscopy, showing that the feldspar framework of celsian begins to be established by about 500°C but the Ba is still moving into its polyhedral lattice sites about 400°C after the sluggish onset of crystallization. Lanthanum hexaluminate and YAG crystallise sharply at 1230 and 930°C respectively, the former via  $\gamma\text{-Al}_2\text{O}_3$ , the latter via  $\text{YAlO}_3$ . Yttrium moves into the garnet lattice sites less than 100°C after crystallisation.

**Key words :** Gels, Masnmr, Lanthanumhexaluminate, Celsian, YAG

### I. Introduction

Fibre-reinforced ceramic composites consist of a matrix material, the fibres and possibly one or more layers of fibre-coating material whose purpose is to permit only weak bonding of the fibre to the matrix, allowing efficient crack deflection and fibre pullout. Our goal is to develop composites for use in high-temperature oxidising conditions, suggesting the preferred use of oxides as the matrix and fibres.

The desirable properties of the fibre/matrix interface material for oxide-oxide composites are that it should have long-term stability in high-temperature oxidising environments, it should bond only weakly with either the fibre or the matrix material, or that it should contain crystallographic cleavage planes which can be oriented parallel to the fibre-matrix interface. A number of simple and complex oxides have been suggested<sup>1</sup> as candidates for the interface layer in oxide-oxide composites. Of these, hexagonal celsian,  $\text{BaAl}_2\text{Si}_2\text{O}_8$ , is a potentially useful interface phase, since this crystalline modification undergoes a polymorphic phase transformation at 300°C, with an associated volume change which can lead to the mechanical instability which is useful in an interface material to minimise bonding between the fibres and the matrix. Hexacelsian is a feldspar with a structure consisting of tetrahedral Al,Si double-layers with the larger Ba ion in

the polyhedral sites between the double layers (Fig. 1A). Lanthanum hexaluminate may be another useful interface candidate, since it has the magnetoplumbite structure<sup>2</sup> related to  $\beta$ -alumina, consisting of alumina spinel blocks separated by mirror planes containing the  $\text{La}^{3+}$  (Fig. 1B). The present study of the sol-gel preparation and properties of hexacelsian and lanthanum hexaluminate fibre coatings was undertaken in the context of a larger project to develop fibre-reinforced composites based on mullite ( $\text{Al}_2\text{Si}_2\text{O}_7$ ). The scope of the present work was also broadened to include yttrium aluminium garnet (YAG,  $\text{Y}_3\text{Al}_5\text{O}_{12}$ ), a potentially interesting matrix material which might also have properties suitable for the interface region. The cubic garnet structure of YAG contains octahedral and tetrahedral sites, both occupied by Al, with the larger Y atoms surrounded by 8 oxygens in a dodecahedral site (Fig. 1C).

The soft (low-temperature) chemical approach of sol-gel synthesis has considerable advantages as a method for producing the matrix and fibre elements of oxide/oxide composites, since their homogeneity allows them to transform to crystalline ceramics at relatively low temperatures, and fibres may be spun from suitable gel solutions. The interface phases can also be conveniently prepared from gel precursors, which can be applied by dip-coating or drawing the fibres through a gel bath. The thermal evolution of crystalline products from these gel-

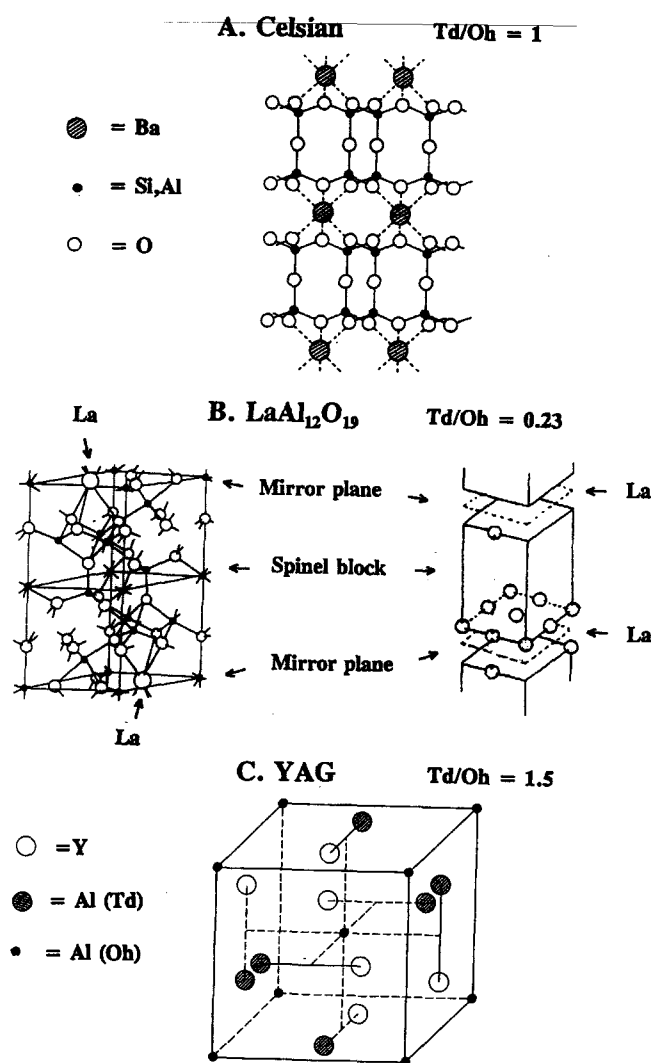


**Fig. 1.** Structures of: A. Hexagonal celsian, B. Lanthanum hexaluminate, C. Yttrium aluminium garnet (YAG).

derived precursors involves several steps, including the removal of solvent and volatile by-products and the atomic rearrangements necessary to establish the crystal structure. Solid state nuclear magnetic resonance spectroscopy with magic-angle spinning (MAS NMR) has proved to be a useful technique for studying the atomic arrangements in gel-derived ceramic precursors prior to their crystallization. The present work uses a combination of MAS NMR, thermal analysis and X-ray powder diffraction to study the thermal evolution of crystalline hexacelsian, lanthanum hexaluminate and YAG from hybrid (organic/inorganic) gels of the appropriate compositions.

## II. Experimental

The gels were prepared from reagent grade Al-sec-butoxide, tetraethylorthosilicate (TEOS), and the acetates of Ba, La and Y as appropriate. The celsian gel was prepared by the method of Tredway and Risbud<sup>3)</sup>

involving the slow addition of a dilute solution of Al-sec-butoxide in isopropanol to partially-hydrolysed TEOS in ethanol followed by the addition of an aqueous solution of Ba acetate acidified with acetic acid. After gelation, the product was dried slowly to allow the volatilization of the alcohol by-products. The YAG gel was similarly prepared from Al-sec-butoxide in isopropanol and aqueous Y acetate solution by the method of Gowda.<sup>4)</sup> Several different methods for the preparation of lanthanum hexaluminate were tried; the results reported here are for a gel prepared from a solution of Al-sec-butoxide in 2-propanol, stabilised by adding 38 mol% acetylacetonate (AcAc). La acetate was dissolved in this solution with vigorous stirring under an Ar atmosphere to prevent premature hydrolysis, and the mixture peptized with HNO<sub>3</sub>. Gelation was carried out in air at 60°C, followed by vacuum drying at 40-60°C.

Thermal analysis was carried out on the dried gels in flowing air (50 ml·min<sup>-1</sup>) at a heating rate of 10°C min<sup>-1</sup> using a Rheometrics STA 1500 thermoanalyser. Powdered samples of the gels were heated separately to various temperatures in platinum crucibles for 15 min (celsian and YAG) or for 60 min (lanthanum hexaluminate) in a pre-heated electric muffle furnace, then examined by XRD (Philips PW1700 computer-controlled goniometer with a graphite monochromator and Co K $\alpha$  radiation) and by multinuclear MAS NMR spectroscopy at a field strength of 11.7T (Varian Unity 500 spectrometer with 5 mm Doty MAS probe spun at 10-12 kHz). The NMR acquisition conditions were:

<sup>27</sup>Al: spectra acquired at 130.245 MHz using a 15° pulse of 1  $\mu$ s and a recycle time of 1s, the spectra referenced to Al(H<sub>2</sub>O)<sub>6</sub><sup>3+</sup>.

<sup>29</sup>Si: spectra acquired at 99.297 MHz using a 90° pulse of 6  $\mu$ s and a recycle time of 60s, the spectra referenced to tetramethylsilane (TMS).

<sup>137</sup>Ba: spectra acquired at 55,541 MHz using a Hahn spin echo pulse sequence with 16-step phase recycling and a refocussing interval of 20  $\mu$ s, the spectra referenced to 1M aqueous BaCl solution. Approximately 500,000 transients were acquired for each spectrum, which was processed by left-shifting by 2 points to minimise the effects of probe ringdown, pulse breakthrough, etc.

<sup>89</sup>Y: spectra acquired at 24.5 MHz using the Hahn spin echo pulse sequence as above. Since the relaxation delay times of some 89Y compounds are known to be long in the absence of deliberately introduced paramagnetic species, a recycle delay of 3000s was used here, with typically 60 transients acquired. The spectra were baseline-corrected and referenced to aqueous YCl<sub>3</sub> solution.

## III. Results and Discussion

The differential scanning calorimetric (DSC) curves of the three dried gels are shown in Fig. 2.

All the gels lose volatile constituents (solvents and

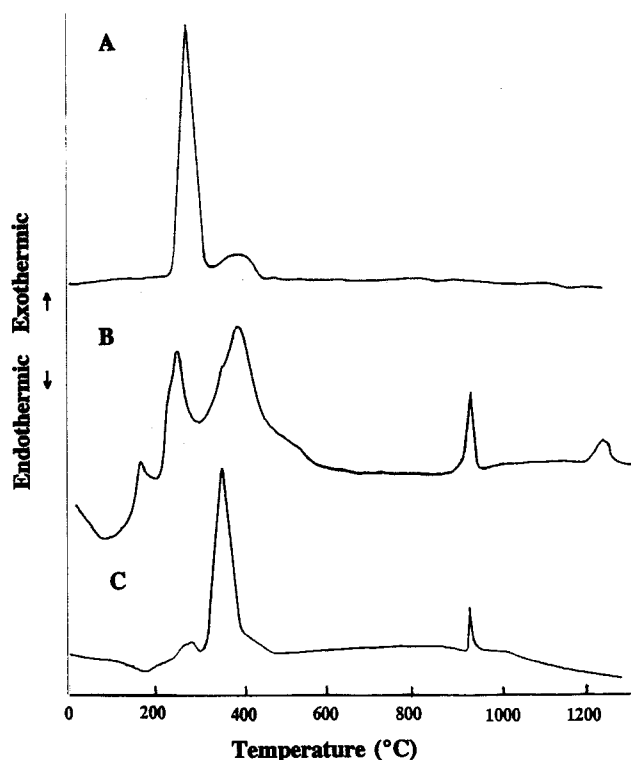


Fig. 2. DSC traces of: A. Celsian gel, B. Lanthanum hexaluminate gel, C. Yttrium aluminium garnet gel. Heating rate  $10^{\circ}\text{C min}^{-1}$  in air ( $50 \text{ ml} \cdot \text{min}^{-1}$ ).

alcohol by-products) in more than one stage below about  $450^{\circ}\text{C}$ ; these events are exothermic because they involve the pyrolytic oxidation of organic species. The total mass losses associated with the  $<450^{\circ}\text{C}$  exotherms in celsian, lanthanum hexaluminate and YAG are 40.9%, 60% and 47% respectively. After the exothermic loss of the organics, all three gels remain X-ray amorphous. The DSC of celsian gel (Fig. 2A) shows no further thermal events up to  $1300^{\circ}\text{C}$ , but the lanthanum hexaluminate gel shows a sharp exotherm at  $936^{\circ}\text{C}$  and a broader exotherm at  $1237^{\circ}\text{C}$  (Fig. 2B). The YAG gel shows a sharp exotherm at  $930^{\circ}\text{C}$  (Fig. 2C). These higher-temperature events have no associated mass change, and are related to the crystallization process.

XRD shows that despite the lack of a crystallization exotherm in the celsian gel, crystallization occurs sluggishly over the temperature range  $900\text{--}1100^{\circ}\text{C}$  (Fig. 3); at  $900^{\circ}\text{C}$ , the major reflection of celsian has begun to develop on the side of the major broad amorphous gel XRD hump. At the same temperature, peaks corresponding to the major reflections of mullite ( $\text{Al}_6\text{Si}_2\text{O}_{13}$ ) and BaO appear, suggesting the presence of inhomogeneous aluminosilicate and Ba-rich regions in the gel, possibly resulting from phase separation. By  $1100^{\circ}\text{C}$  these have given way to well-crystallised celsian, with very small traces of  $\text{Ba}_2\text{SiO}_4$  and  $\text{BaAl}_2\text{O}_4$ , the latter disappearing only slowly on heating to  $1250^{\circ}\text{C}$ .

The XRD patterns of lanthanum hexaluminate (Fig. 4)

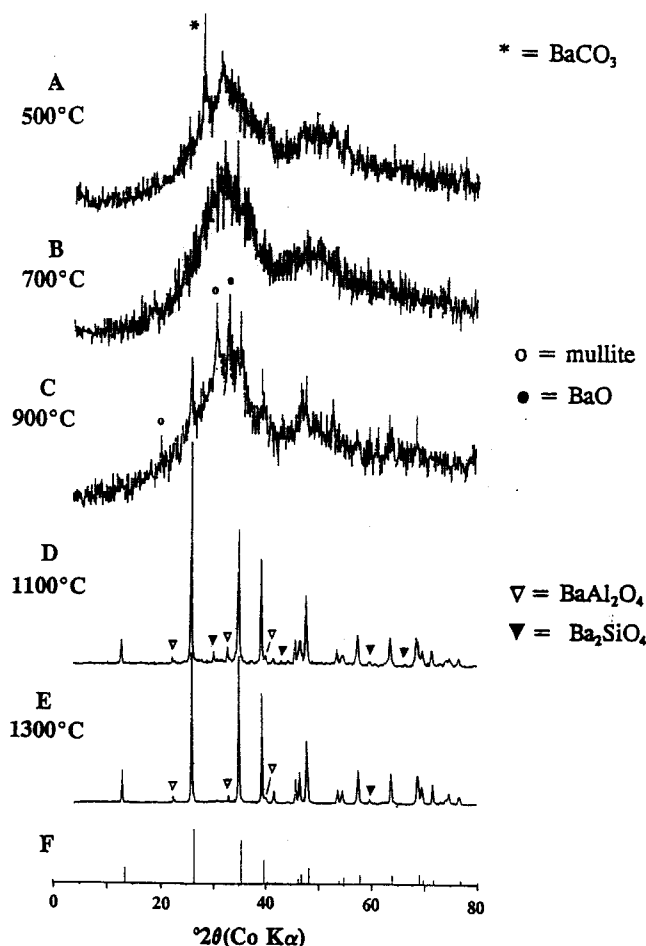


Fig. 3. XRD traces of celsian gel heated at the indicated temperatures for 15 min. The powder pattern of hexagonal celsian (PDF no. 28-124) is shown in F.

show the development of diffuse lines above the temperature of the  $936^{\circ}\text{C}$  exotherm, corresponding to  $\gamma\text{-Al}_2\text{O}_3$  (PDF pattern no. 10-425, indicated by asterisks in Fig. 4D). The spinel structure of  $\gamma\text{-Al}_2\text{O}_3$  appears to be stabilised by the presence of the La up to about the temperature of the second exotherm, when the diffuse pattern changes abruptly to that of hexagonal  $\text{LaAl}_{11}\text{O}_{18}$  (PDF no. 33-699, shown in Fig. 4G). At  $1200^{\circ}\text{C}$  some of the peaks of the latter phase, notably the major 017 reflection at  $d=2.64 \text{ \AA}$ , are broad and poorly developed (Fig. 4E). Heating at  $1350^{\circ}\text{C}$  produces a sharper pattern (Fig. 4F), but a small trace of crystalline  $\alpha\text{-Al}_2\text{O}_3$  is also detectable at this temperature, resulting from the transformation of a slight excess of  $\gamma\text{-Al}_2\text{O}_3$  probably resulting from the known non-stoichiometry of the final product.<sup>10</sup>

The XRD patterns of YAG (Fig. 5) change abruptly from the broad, amorphous gel trace to a crystalline material at about the exotherm temperature (Fig. 5C). The initial crystallization products from the YAG gel are a mixture of YAG and hexagonal  $\text{YAlO}_3$ , indicated by asterisks in Fig. 5C) but the latter is completely converted to YAG by  $1000^{\circ}\text{C}$  (Fig. 5D). The appearance of an

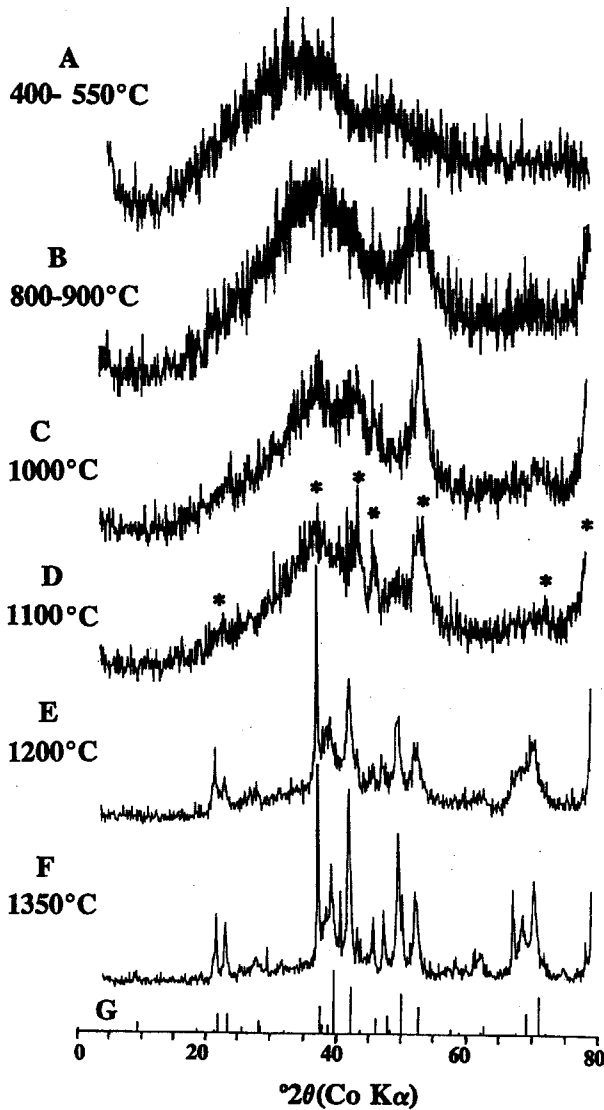


Fig. 4. XRD traces of lanthanum hexaluminate gel heated at the indicated temperatures for 60 min. Asterisks indicate the reflections of  $\gamma\text{-Al}_2\text{O}_3$  (PDF no. 10-425). The powder pattern of  $\text{LaAl}_{11}\text{O}_{18}$  (PDF no. 33-699) is shown in G.

intermediate phase in the crystallization of YAG from its gel is unusual, having been previously reported only in metal diphasic metal isopropoxide gels<sup>6</sup>; the present transitory appearance of  $\text{YAlO}_3$  may thus indicate a slight degree of inhomogeneity.

### 1. $^{27}\text{Al}$ MAS NMR Spectroscopy

The  $^{27}\text{Al}$  MAS NMR spectra of celsian gels show a predominance of octahedral Al in the unheated gel (Fig. 6), in which the two peaks in the octahedral region (at -11 and -32 ppm) arise from a single site acted on by an electric field gradient (EFG) due to site distortion which gives rise to a typical quadrupolar lineshape. This lineshape can be simulated by allowing the nuclear quadrupole coupling constant and the asymmetry parameter to take the values of 7.8 MHz and 0.2 respectively (Fig. 6A,

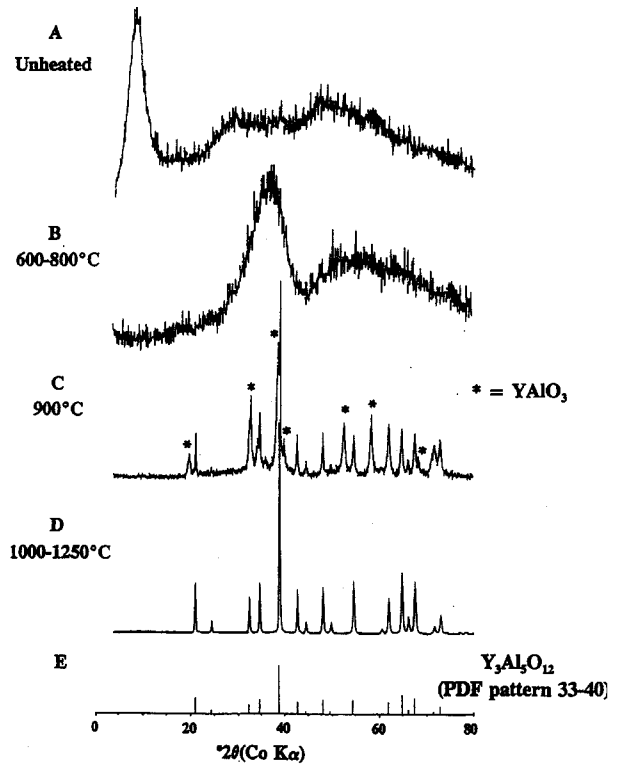


Fig. 5. XRD traces of YAG gel heated at the indicated temperatures for 15 min.

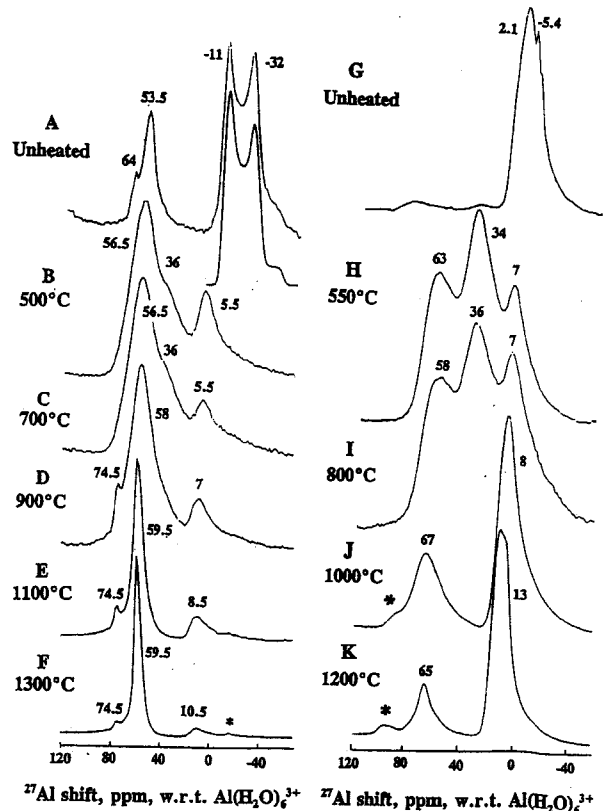


Fig. 6. 11.7T  $^{27}\text{Al}$  MAS NMR spectra of: A-F. celsian gel, G-K. Lanthanum hexaluminate gel, heated at the indicated temperatures for 15 min. Asterisk indicates spinning side bands.

insert). The resulting calculation indicates that the isotropic chemical shift (the chemical shift in the absence of the EFG) is -0.5 ppm, close to the value of the hydrated Al ion used as the reference for these spectra.

Heating the gel produces a progressive increase in the proportion of the tetrahedral Al resonance at about 60 ppm, as the tetrahedral Al(Si)-O feldspar framework is slowly established. Between about 500-800°C, a broad shoulder at about 36 ppm appears, in the position often attributed to Al in five-fold coordination. An alternative explanation which appears to be valid for aluminosilicate gels of mullite composition,<sup>6</sup> ascribes this resonance to a relaxed form of a characteristic defect tetrahedral oxygen tricluster defect. In the present gels, this shoulder may be accounted for by the formation of some mullite-like units, as revealed at higher temperatures by XRD. The smaller tetrahedral and octahedral peaks, at 74.5 and about 8 ppm respectively, decrease with heating temperature, suggesting that they arise from intermediate phases (the 74.5 ppm peak coincides with that of  $\text{BaAl}_2\text{O}_4$ , which is known from XRD to persist in small amounts). The changes in the relative population of the Al sites during heating, as deduced by curve-fitting the  $^{27}\text{Al}$  NMR spectra, are shown in Fig. 7A.

The  $^{27}\text{Al}$  MAS NMR spectrum of the unheated lanthanum hexaluminate gel indicates that the Al is present predominantly in octahedral sites (2.1 and -5.4 ppm, Fig. 6G). Despite the broadness of this resonance, partial resolution of at least two peaks can be observed, the lineshapes of which suggest multiple sites rather than a quadrupole profile. Heating to 550°C converts a significant proportion of the octahedral sites to tetrahedral and the 34 ppm site which may represent either penta-coordinate Al or tricluster defect sites. The mechanism for tricluster formation as a charge-compensation mechanism can readily be understood in aluminosilicate tetrahedra<sup>6</sup> but is less easily envisaged in Si-free systems especially where the other cations (La or Y) are too large to enter into the tetrahedral network. The gel may therefore consist of an amorphous aluminate network containing irregularly cross-linked tetrahedral/octahedral clusters. Tricluster formation may be necessary to provide a localised charge compensation mechanism in the regions where the relatively large and immobile rare earth ion is too remotely located to carry out this function.

As was found for celsian, the intensity of the 36 ppm resonance decreases abruptly and disappears altogether at 1000°C (Fig. 6J); by contrast with celsian, however, this corresponds to the formation of  $\gamma\text{-Al}_2\text{O}_3$  spinel, and is well below the temperature at which crystalline  $\text{LaAl}_{11}\text{O}_{18}$  appears. Most of the Al from the 36 ppm sites finds its way into the octahedral sites (Fig. 7B) such that at the appearance of crystalline  $\text{LaAl}_{11}\text{O}_{18}$  (Fig. 6K) the measured tetrahedral/octahedral ratio is 0.24, in excellent agreement with the value of 0.23 expected from the crystal structure.

The  $^{27}\text{Al}$  NMR spectrum of unheated YAG gel indicates

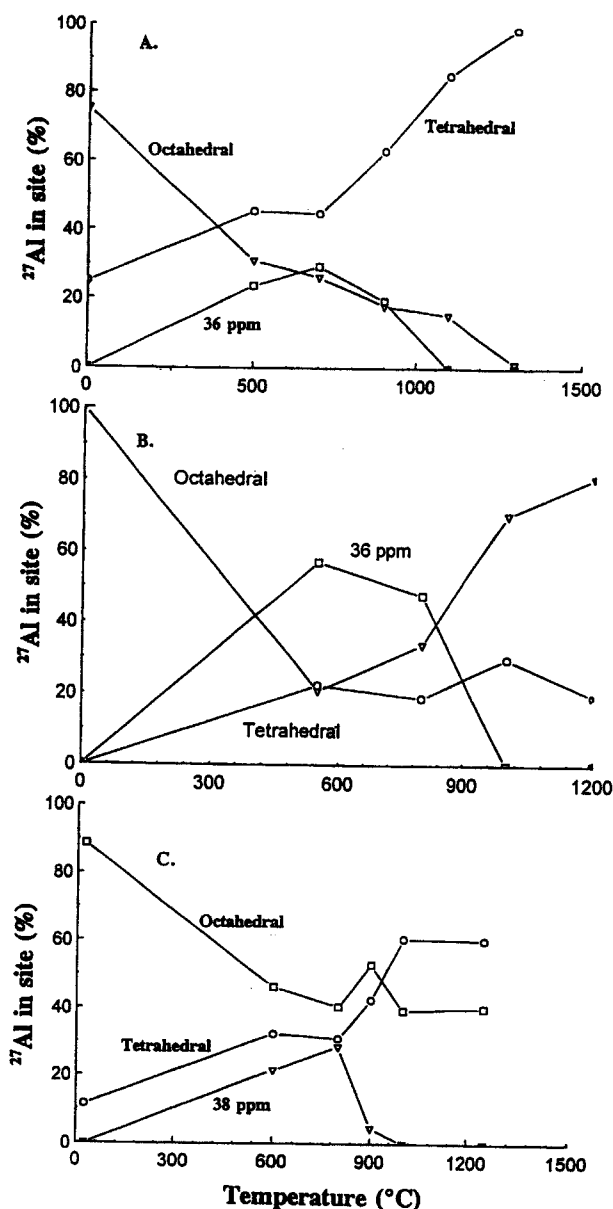


Fig. 7. Changes in the  $^{27}\text{Al}$  site occupancies as a function of heating temperature. A. Celsian gel, B. Lanthanum hexaluminate gel, C. YAG gel.

that the Al is principally in octahedral sites (at about 7 ppm), with only a hint of tetrahedral Al present (Fig. 8A). After expulsion of the volatiles <600°C, a three-peak spectrum appears (Fig. 8B), similar to that found in the  $\text{LaAl}_{11}\text{O}_{18}$  gels. This spectrum persists to within 100°C of the crystallisation temperature, when it abruptly disappears, leaving only tetrahedral and octahedral (0.8 ppm) sites (Fig. 8C). The plot of site occupancy as a function of heating temperature (Fig. 6C) indicates a transitory increase in the octahedral occupancy at this temperature; this coincides with the brief appearance of hexagonal  $\text{YAlO}_3$ , a phase which has been suggested to contain 5-coordinated Al,<sup>7</sup> but whose NMR spectrum has not been reported. The possible incipient formation of  $\text{YAlO}_3$  in

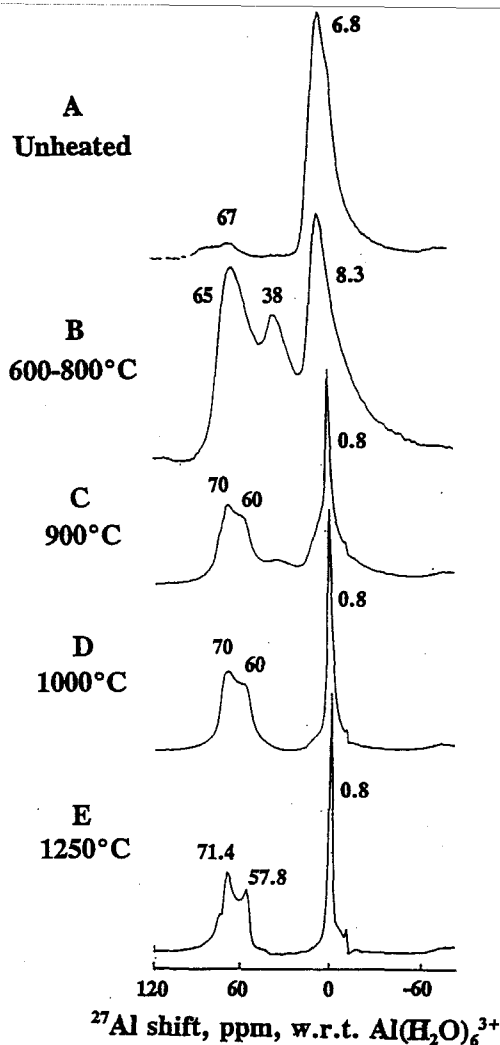


Fig. 8. 11.7T  $^{27}\text{Al}$  MAS NMR spectra of YAG gel heated at the indicated temperatures for 15 min.

the YAG gels at lower temperatures does not however provide a satisfactory explanation for the 38 ppm in terms of 5-fold coordinated Al, since the 38 ppm peak has practically disappeared in the sample containing crystalline  $\text{YAlO}_3$  (Fig. 8C). The tetrahedral and octahedral resonances of YAG become sharper on heating to higher temperatures (Fig. 8E). The tetrahedral site shows a distinctive quadrupole splitting due to the presence of an EFG. The quadrupolar lineshape can be simulated by using previously reported values for the nuclear quadrupole coupling constant and asymmetry factor of 6 MHz and 0 respectively, yielding an isotropic chemical shift of 76.5 ppm for this site. A similar calculation shows the EFG at the octahedral site to be much smaller, corresponding to a nuclear quadrupole coupling constant of 0.6 MHz. The Al site occupancies derived from the  $^{27}\text{Al}$  NMR spectrum of YAG at 1200°C indicate a tetrahedral/octahedral ratio of 1.5, in excellent agreement with the ratio expected from the crystal structure.

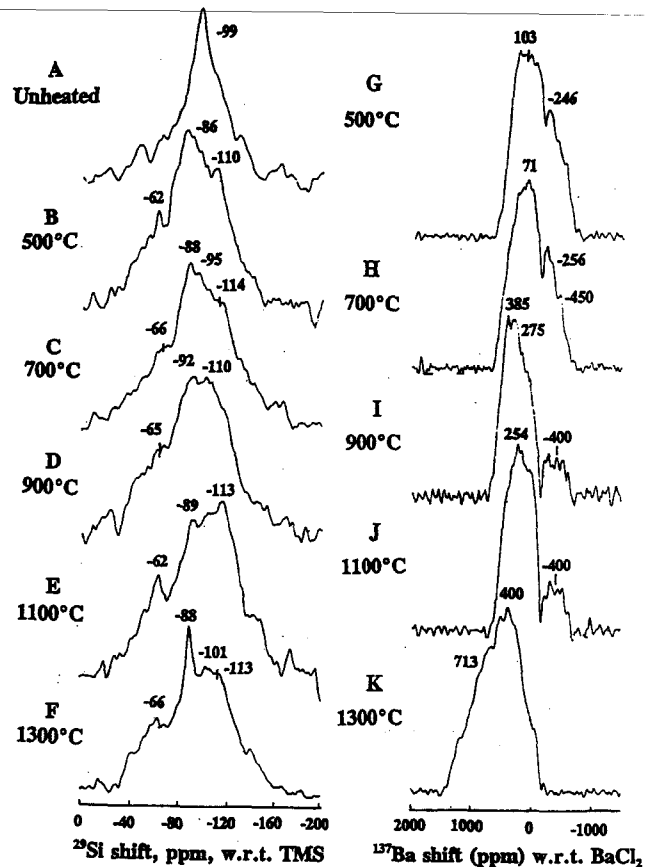


Fig. 9. 11.7T MAS NMR spectra of celsian gel heated at the indicated temperatures for 15 min. A-F.  $^{29}\text{Si}$  spectra, G-K.  $^{137}\text{Ba}$  spectra.

## 2. $^{29}\text{Si}$ , $^{137}\text{Ba}$ and $^{89}\text{Y}$ MAS NMR Spectroscopy

Since the present samples contain other elements whose nuclei are suitable for NMR study, their NMR spectra were also obtained in order provide additional information about the gel transformations in these compounds.

The NMR spectra of both  $^{29}\text{Si}$  and  $^{137}\text{Ba}$  acquired for the unheated and heated celsian gels (Fig. 9) are broad and somewhat featureless. Soon after expulsion of the volatiles <500°C, the  $^{29}\text{Si}$  spectrum acquires the essential features of the tetrahedral feldspar framework (the poorly resolved group of resonances at about -86 ppm to -113 ppm). The development of crystalline celsian is characterised principally by the increasing importance of the resonance at -88 ppm associated with  $\text{Q}^4$  (4Al) sites (tetrahedral Si with four Al nearest neighbours). The spectral intensity in the region of -113 ppm is associated with the  $\text{Q}^4$  (0Al) sites of uncombined  $\text{SiO}_2$  and is sometimes found in natural feldspars in which it is attributed to XRD-undetectable silica impurities in the grain boundaries. Another  $^{29}\text{Si}$  resonance at -62 to -66 ppm which appears at 500°C and remains throughout the heating process arises from the presence of incipient  $\text{Ba}_2\text{SiO}_4$ . This phase appears in small amounts in the XRD trace and is still present at 1300°C.

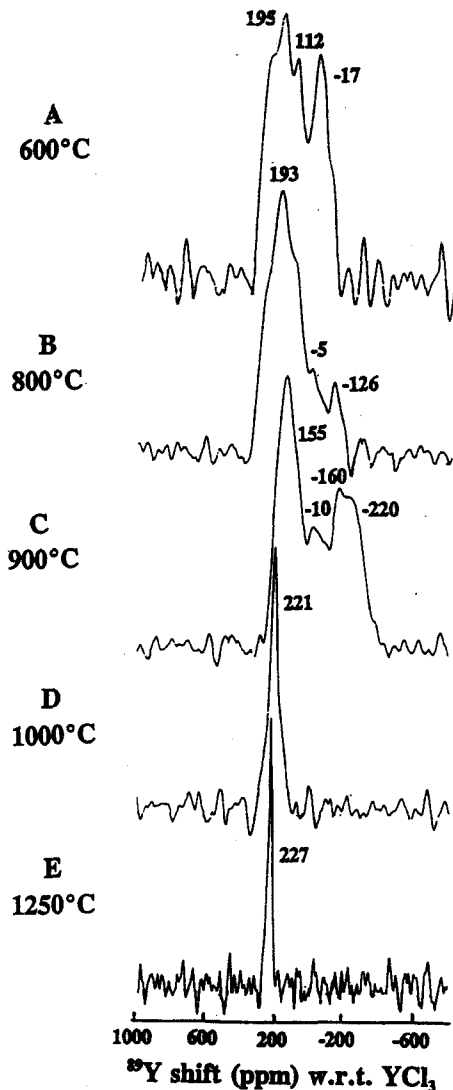


Fig. 10. 11.7T  $^{89}\text{Y}$  MAS NMR spectra of YAG gel heated at the indicated temperatures for 15 min.

The  $^{137}\text{Ba}$  spectra of the gels (Fig. 9) show a progressive shift in the centre-of-gravity (COG) of the broad resonance envelope from about 70 to 250 ppm at 900°C. The broad envelope contains the unresolved resonances of the Ba species known by XRD to be present at various stages of the thermal reaction sequence, namely  $\text{BaCO}_3$  (386 and -406 ppm),<sup>8)</sup>  $\text{Ba}_2\text{SiO}_4$  (COG -270 ppm)<sup>9)</sup> and  $\text{BaAl}_2\text{O}_4$  (COG -191 ppm).<sup>8)</sup> The major shift of the gel COG towards the less shielded position of celsian (COG >> 600 ppm) occurs late in the thermal sequence (1300°C), indicating that the large Ba ion moves into its final coordination polyhedron of 9 oxygen nearest neighbours well after the establishment of the feldspar aluminosilicate framework.

The  $^{89}\text{Y}$  spectra of the YAG gels (Fig. 10) show generally similar features to the  $^{137}\text{Ba}$  spectra of celsian gels. The broadness of the spectra at lower temperatures is as expected for Y in a number of sites of slightly different environments. In the sample heated at 900°C, the broad-

ness of the resonance envelope probably masks the narrow peak at 214.7 ppm of  $\text{YAlO}_3$ ,<sup>9)</sup> known to co-exist with YAG in this sample. By contrast with the behaviour of Ba in celsian, crystallization of YAG is accompanied by an immediate narrowing of the Y resonance and its shift to the less shielded position expected for YAG (222 ppm),<sup>9)</sup> suggesting that it achieves its final environment less than 100°C higher than the temperature at which the YAG structure is established.

#### IV. Conclusions

(1) Multinuclear solid-state MAS NMR results are useful in complementing thermal analysis and XRD studies of gel crystallization reactions, by providing information about changes in the atomic environments in the gels prior to crystallization.

(2) The combined data for hexacelsian gels indicates that the Si atoms assume the essential features of a typical feldspar framework soon after the expulsion of the volatiles at about 500°C. Al occupies the tetrahedral feldspar sites more gradually, and Ba migrates into its final 9-fold coordinated polyhedra well after the establishment of the long-range ordering of feldspar is indicated by XRD.

(3) The present lanthanum hexaluminate gel remains X-ray amorphous until an exothermic event at 936°C which accompanies the formation of the cubic  $\alpha\text{-Al}_2\text{O}_3$  spinel component. The associated conversion of octahedral Al to tetrahedral involves an intermediate coordination state characterized by a  $^{27}\text{Al}$  NMR resonance at 36 ppm. By 1200°C, when the characteristic XRD pattern of  $\text{LaAl}_{11}\text{O}_{18}$  abruptly appears, the tetrahedral/octahedral Al ratio has assumed the value demanded by the crystal structure.

(4) The present amorphous YAG gel crystallizes abruptly at about 900°C to  $\text{YAlO}_3$ , which completely converts to YAG below 1000°C. As in  $\text{LaAl}_{11}\text{O}_{18}$ , the progressive conversion of octahedral Al to tetrahedral below the crystallization temperature involves the intermediate appearance of Al in sites characterized by a  $^{27}\text{Al}$  NMR resonance at 38 ppm which disappears abruptly at the appearance of crystalline  $\text{YAlO}_3$ . The Y moves more slowly to its final crystal environment; this is however achieved within 100°C of the XRD appearance of YAG.

#### References

1. P. E. D. Morgan and D.B. Marshall, "Functional Interfaces for Oxide/oxide Composites," *Mater. Sci. Eng., A* **162**, 15-25 (1993).
2. N. Iyi, S. Takekawa and S. Kimura, "Crystal Chemistry of Hexaaluminates:  $\beta$ -alumina and Magnetoplumbite Structures," *J. Sol. State Chem.*, **83**, 8-19 (1989).
3. W. K. Tredway and S. H. Risbud, "Gel Synthesis of Glass Powders in the  $\text{BaO-Al}_2\text{O}_3\text{-SiO}_2$  System," *J. Non-Cryst. Solids.*, **100**, 278-283 (1988).
4. G. Gowda, "Synthesis of Yttrium Aluminates by the sol-gel Process," *J. Mater. Sci. Lett.*, **5**, 1029-1032, (1986).

5. R. S. Hay, "Phase Transformations and Microstructure Evolution in Sol-gel Derived Yttrium-aluminium Garnet Films," *J. Mater. Res.*, **8**, 578-604 (1993).
6. M. Schmucker and H. Schneider, "A New Approach on the Coordination of Al in Non-crystalline Gels and Glasses of the System  $\text{Al}_2\text{O}_3\text{-SiO}_2$ ," *Ber. Bunsenges Phys. Chem.*, **100**, 1550-1553 (1996).
7. R. Dupree, M. H. Lewis and M. E. Smith, "Structural Characterization of Ceramic Phases with High-resolution  $^{27}\text{Al}$  NMR," *J. Appl. Cryst.*, **21**, 109-116 (1988).
8. K. J. D. MacKenzie and R. H. Meinhold, "Prospects for  $^{137}\text{Ba}$  MAS NMR Spectroscopy of Ceramics and Related Inorganic Materials," *Ceram. Int.*, (in press).
9. R. Dupree and M. E. Smith, "Structural Influences on High-resolution Yttrium-89 NMR Spectra of Solids," *Chem. Phys. Lett.*, **148**, 41-44 (1988).
10. N. Iyi, Z. Inoue, S. Takekawa and S. Kimura, "The Crystal Structure of Lanthanum Hexaluminate," *J. Sol. State Chem.*, **54**, 70-77 (1984).